

NJ

GPO PRICE \$ \_\_\_\_\_

CFSTI PRICE(S) \$ \_\_\_\_\_

Hard copy (HC) 300

Microfiche (MF) 65

ff 653 July 65

## SOLAR CELL RADIATION EXPERIMENT ON THE EXPLORER XXIII

### MICROMETEOROID SATELLITE

By Walter E. Ellis and James Bene

NASA Langley Research Center  
Langley Station, Hampton, Va.

Presented at the Virginia Academy of Sciences' Annual Meeting

Norfolk, Virginia  
May 5-6, 1967

N 68-27541

FACILITY FORM 602	(ACCESSION NUMBER)	(THRU)
	28	
	(PAGES)	
	TMX-60138	
	(NASA CR OR TMX OR AD NUMBER)	(CODE)
		03
		(CATEGORY)

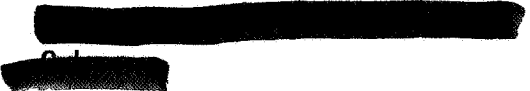
NASA - Langley

SOLAR CELL RADIATION EXPERIMENT ON THE EXPLORER XXIII  
MICROMETEOROID SATELLITE

By Walter E. Ellis and James Bene

Abstract of Paper Proposed for  
Virginia Academy of Sciences' Annual Meeting  
May 5-6, 1967  
Norfolk, Virginia

Shielded and unshielded, N/P, 1 ohm-cm, silicon solar cells were monitored for radiation damage during 1 year in orbit on the Explorer XXIII Micrometeoroid Satellite by measuring their output voltages while operating into fixed resistive loads. The orbital parameters were 464 km perigee, 980 km apogee, 51.9° inclination, and 99.2 minutes orbital period. No significant degradation was experienced during the first 79 days after launch. Thereafter, damage plateaus were observed, with more rapid degradation occurring during the periods when apogee was in the southern hemisphere. After 1 year, solar cells shielded with 0.476 cm-thick fused silica had degraded 4 percent, and unshielded cells had degraded 16 percent. A solar aspect sensor, employing 6 solar cells arranged in a hexagonal configuration, and shielded with 0.636 cm-thick fused silica, also degraded approximately 4 percent.



O.I.

# SOLAR CELL RADIATION EXPERIMENT ON THE EXPLORER XXIII

## MICROMETEOROID SATELLITE

Walter E. Ellis and James Bene

### INTRODUCTION

The presence of energetic electrons and protons trapped in the earth's magnetic field presents a hazard to man's exploration of space, both to personnel in manned missions, and to certain materials and components used in the construction and operation of the spacecraft. Solar cells, widely used on spacecraft to convert sunlight to electrical power, are particularly vulnerable to these energetic particles. Transparent shields are almost universally used in solar cell space power systems to provide some protection from particulate irradiation. Weight considerations, however, often limit the amount of shielding that can be effectively employed.

The objective of the solar cell radiation damage experiment on the Explorer XXIII satellite was to determine the effects of particulate irradiation on the performance of shielded and unshielded silicon solar cells while operating in the near-earth environment. This was accomplished by monitoring their output voltages while they were operating in space into fixed resistive loads, and comparing the results with initial voltages obtained from ground calibrations, and from flight data received soon after injection into orbit.

### Description of Satellite

The Explorer XXIII micrometeoroid satellite, figure 1, was launched from Wallops Station on November 6, 1964, by means of a Scout vehicle. It was injected into an elliptical orbit with a perigee altitude of 464 km and

an apogee altitude of 980 km. The angle of inclination was 51.95° and the orbital period was 99.23 minutes. Its primary objective was to obtain statistical data on the meteoroid hazard in near-earth space. This was accomplished by measuring the meteoroid penetrations of two thicknesses of stainless steel used as exposed surfaces on pressurized cells.

Electric power for the telemetry and other electronic systems was supplied from solar cells and nickel-cadmium batteries. The power solar cell modules were located on the periphery of the nose section and on the forward surface of the spacecraft.

#### Description of Experiment

The radiation damage experiment consisted of a solar aspect sensor and four solar cell test groups. These components were located in the same plane on the forward surface of the spacecraft. The silicon solar cells were 1 by 2 cm, N on P, with 1.0 ohm-cm base resistivity, and were the same type of cells as used in the primary power system. The aspect sensor provided the solar orientation data necessary to evaluate the data received from the test groups.

Figure 2 shows a simplified drawing of the solar aspect sensor. It consisted of six triangular solar cell segments arranged in a hexagon, with an effective area of  $2.49 \text{ cm}^2$ . Each segment was loaded with a 22-ohm, wire-wound, low-temperature-coefficient resistor. These resistors were series connected to provide an output voltage that was compatible with the telemetry system. The sensor was shielded with a synthetic fused silica cover, 0.636 cm (1/4-inch) thick, which provided a transparent window 1.67 cm in diameter centered over the solar cells.

Figure 3 shows a simplified drawing of test groups 1 and 2. These were shielded with 0.476 cm (3/16-inch) thick synthetic fused silica in the same manner as the solar cells on the primary power system. Groups 3 and 4 were mounted in the same manner but without any shielding. The five cells in each group were series-connected into a shingled configuration, and operated into a fixed load of 33 ohms. This was an optimum load, determined from laboratory tests, to provide an initial output voltage of approximately 1.9 volts at normal incidence space-sun illumination, and to maximize linearity as a function of illumination intensity.

Figure 4 shows the normalized angular response of the aspect sensor as determined from ground calibrations. This curve represents the response as measured with incident illumination at angles from  $0^\circ$  to  $\pm 90^\circ$ . The maximum deviation from this curve of measurements made at roll angles from  $0^\circ$  to  $180^\circ$  was less than  $\pm 2$  percent. Because of its unique design, and the method of loading employed, the angular response of the aspect sensor differed considerably from the familiar cosine curve in that the slope of the curve as shown is more linear, resulting in a more accurate determination of the angle of solar incidence.

Figure 5 shows the normalized angular responses of the test solar cell groups. These are the average responses of the two shingles in each group as measured with incident illumination at angles from  $0^\circ$  to  $\pm 90^\circ$ . It can be observed that, at angles greater than  $50^\circ$ , the shielded groups exhibit a lower response, resulting in a lower cut-off angle because of shadows caused by the shield retainer ring.

Several factors influenced the magnitude of output voltages from the aspect sensor and the test solar cells, the most influential being the solar angle of incidence at the time of interrogation. Other influencing factors were the variation in solar constant, cell temperatures, and earth-reflected solar radiation.

At injection, the satellite was spinning at a speed of about 2.4 rps. For the day of launch, the angle,  $\eta$ , defined as the angle of the satellite's momentum vector with respect to the sun, was calculated to be about  $26^\circ$ . Figure 6 shows the calculated variation of this angle plotted as a function of time in orbit for 1 year. Assuming a completely stabilized spinning mode, the solar angle of incidence,  $\phi$ , with respect to the solar cells, at injection, would be equal to the angle,  $\eta$ . Within a few days after injection, the longitudinal axis of the spacecraft would normally be expected to begin to cone as the spin rate decreased. The cone angle would normally enlarge with time, developing into a full  $90^\circ$  tumble several months later. After the satellite had attained a full  $90^\circ$  tumble mode, and disregarding all influencing factors acting upon the spacecraft, the angle,  $\phi$ , would normally be expected to become  $0^\circ$  at approximately 6 month intervals, because of the rotational movement of the earth with respect to the sun. However, as will be shown later, the angle,  $\phi$ , became  $0^\circ$ , and maximum output voltages occurred at irregular intervals during the year.

Figure 7 shows the percentage deviation of the solar constant from a mean value of  $140 \text{ mW/cm}^2$  for a 1-year period after launch, reference 1. The maximum deviation is shown to be  $\pm 3.4$  percent.

In addition to the temperature dependent factors considered in the design of the spacecraft, and the thermal controls employed, the flight temperatures of the solar cells were also dependent upon the sunlight-to-darkness ratio for each orbit, and the time interval between the emergence of the spacecraft from the earth's penumbra and the time of interrogation. The temperatures experienced by the solar cells during the 1 year in orbit ranged from a maximum of 40° C to a minimum of -5° C. From pre-flight calibrations, it was determined that, over this temperature range, the temperature-induced variations in cell voltages would be within the limitation of data accuracy of the telemetry and data read-out systems. Consequently, no temperature corrections were applied to the data.

The earth-reflected solar radiation incident upon a satellite having orbital parameters similar to Explorer XXIII can be as much as 30 percent of direct solar radiation, reference 2. No attempt was made to evaluate the earth-reflected solar radiation during this mission. However, in order to minimize its effect on the results of this experiment, only data were used from those interrogations made while the nose of the spacecraft was oriented away from the earth, that is, near noon local satellite time, and when the solar angle of incidence was less than 40°.

#### RESULTS AND DISCUSSION

Interrogations of 1 minute duration were made during each orbit for the first month, then, three interrogations per day until the end of the mission. These interrogations occurred during both sunlight and darkness periods. However, because of the photovoltaic characteristics of solar cells, only data from those interrogations made during sunlight periods were usable for this experiment.

Figure 8 presents the output voltages of the aspect sensor and one test group for a 12-second interval of data received during a typical interrogation 23 days after launch. The framing rate, that is, the time required to sequentially scan and read all channels of the telemetry system, was approximately 3.6 frames/second for this interrogation. During this interrogation, the spacecraft was coning with a one-half included angle of  $26^{\circ}$ . The voltages passed through minimum and maximum values, with maximum voltages occurring when the solar angle of incidence was a minimum. Because of the small coning angle during this particular orbit, the solar cells were exposed to direct sunlight during the complete coning cycle, resulting in continuous voltage outputs during the entire interrogation. The minimum voltages during each interrogation decreased as the cone angle increased with time, reaching their lowest values about 35 days after launch. After this date, the cone angle was of sufficient magnitude that the solar cells were not in direct sunlight continuously during the coning cycle of the spacecraft.

Figure 9 shows the output voltages received during an interrogation made 230 days after launch. It can be observed that the minimum voltages are relatively constant for an interval during each cycle of cone. The magnitude of the voltages during this interval was dependent upon the intensity of the earth-reflected solar radiation.

The maximum voltages for each orbit increased with time from injection, and reached maximum values corresponding to those expected for zero angle of incidence on the 23rd day after launch. On this date, a study of the cyclic curves indicated that the half-angle of cone was  $26^{\circ}$ , the same as the

angle,  $\eta$ , for that date. This indicated a value of  $0^{\circ}$  for the angle,  $\phi$ . This  $0^{\circ}$  angle of incidence occurred nine additional times during the year at irregular intervals.

Figure 10 shows the normalized output voltage of the aspect sensor for these periods of  $0^{\circ}$  angle of incidence plotted as a function of time in orbit. These voltages gradually decreased with time, and at the end of 1 year, was about 96 percent of the initial voltage. This indicated that the solar cells of the aspect sensor, shielded with 1/4-inch thick synthetic fused silica, degraded about 4 percent of their initial output during the 1 year in space.

This figure also shows the minimum solar aspect angle,  $\phi$ , for selected orbits as indicated by the aspect sensor. The first data point shown is that from orbit 6, on the day of launch. The angle,  $\phi$ , is shown to be  $22^{\circ}$ . As mentioned earlier, the angle,  $\eta$ , on the day of launch was calculated to be  $26^{\circ}$ . This indicated that, approximately 11 hours after injection, the longitudinal axis of the spacecraft was coning with a one-half included angle of  $4^{\circ}$ .

Figure 11 shows the integrated electron flux per orbit for Explorer XXIII for four non-consecutive days during the year. These data were prepared by means of a computer program using space map electron distribution data for 1964. Each bar represents the integrated flux in electrons/cm<sup>2</sup> per orbit for all energies above 0.5 MeV. A total of 15 orbits is shown for each day. However, with an orbital period of 99.23 minutes, each 24-hour period required approximately 14 and one-half orbits. Consequently the average flux rate per day was computed accordingly. The integrated flux per orbit varied by several orders of magnitude.

Table I presents the latitude position of apogee and the average electron flux rate for each of the 4 days for which data were computed. The variation in integrated flux per day approaches one order of magnitude. It is evident that the integrated flux per day and, hence, the solar cell degradation rate, was considerably influenced by the latitude of apogee of the spacecraft.

TABLE I  
ELECTRON FLUX RATE AT VARIOUS LATITUDES OF APOGEE

Date GMT	Latitude of apogee	Integrated flux, electrons/cm <sup>2</sup> -day
311 (1964)	-35°	$3.68 \times 10^{10}$
027 (1965)	-25°	$2.74 \times 10^{10}$
076 (1965)	0°	$2.21 \times 10^{10}$
208 (1965)	+35°	$5.63 \times 10^9$

In figure 12, the latitude of apogee for Explorer XXIII is shown plotted as a function of time in orbit. With an initial perigee of 464 km and an apogee of 980 km, the spacecraft passed through the lower fringe of the radiation belt only during a portion of each orbit. As shown in Table I, the average daily electron flux rate became more appreciable when apogee occurred near the latitudes of the southern anomaly which is centered above the Atlantic Ocean just off the coast of southern Brazil.

Figure 13 shows the variation in the average daily electron flux as a function of time in orbit. This curve was constructed from the flux rates given in Table I, and the latitude of apogee curve in figure 12. It was assumed that the flux rates would be applicable each time apogee occurred at the respective latitudes. The shape and amplitude of the peaks of this curve are uncertain. However, it is believed that the daily flux rate would not change appreciable during the periods when apogee was between  $\pm 35^{\circ}$  and  $\pm 52^{\circ}$  latitude. By integrating the area under the curve, the integrated electron flux for 1 year was calculated to be approximately  $7.6 \times 10^{12}$  electrons/cm<sup>2</sup>, with an average flux rate of  $2.1 \times 10^{10}$  electrons/cm<sup>2</sup>-day.

Figure 14 presents the output voltages from the four solar cell test groups plotted as a function of time for 1 year in space. These voltages were corrected for solar angles of incidence and solar constant variation, and then normalized to their respective initial output voltages. The blank periods in these data were caused by the lack of usable data which resulted from darkness interrogation, large solar aspect angles and erratic telemetry data.

The output voltages from the shielded groups degraded about 4 percent. As shown in figure 10, this is the same percentage degradation as that observed for the shielded aspect sensor. The corresponding degradation of the unshielded groups was about 16 percent. No degradation was observed until about Day 025 GMT, 79 days after launch. The degradation rate was not constant during the year. The relatively rapid decay period occurred when apogee was in the southern hemisphere, and were probably caused by the heavier concentration of trapped electrons and protons at latitudes associated with the South Atlantic anomoly.

As shown in figure 13, the number of electrons with energies above 0.5 MeV that impinged upon the unshielded cells was estimated to be about  $7.6 \times 10^{12}$  electrons/cm<sup>2</sup>-year. Pre-flight electron irradiation tests made on the same type of unshielded cells at several energies from 0.5 MeV to 3.0 MeV indicated that  $7.6 \times 10^{12}$  electrons/cm<sup>2</sup> reduced their maximum power output by about 5 percent as measured under equivalent space sun illumination. These tests also indicated that approximately  $5 \times 10^{13}$  electrons/cm<sup>2</sup> were required to cause 16 percent degradation under similar illumination and loading conditions.

Apparently, a considerable percentage of the degradation experienced by the unshielded cells was caused by protons. From reference 3 it was estimated that the average proton flux rate for Explorer XXIII was approximately  $1.4 \times 10^8$  protons/cm<sup>2</sup>-day. The integrated proton flux for 1 year was estimated to be approximately  $5.1 \times 10^{10}$  protons/cm<sup>2</sup>. Pre-flight proton irradiation tests on similar cells at 22 MeV, and published data on similar cells at 4.6 MeV, reference 4, indicate that an integrated proton flux of  $1 \times 10^{11}$  and  $5 \times 10^{10}$  protons/cm<sup>2</sup>, respectively, was required to cause 11 percent degradation of maximum power measured under equivalent space sun illumination. From these estimates, it appears that about one-third of the damage of the unshielded cells was caused by electrons and the remaining two-thirds resulted from protons.

The degradation experienced by the shielded cells was probably caused by both electrons and protons with energies sufficiently high to penetrate the shield. Based on range-energy relations for silicon-dioxide, electrons with

energies above 2.2 MeV, and protons with energies above 31 MeV should penetrate the 0.476 cm thick shield. However, the percentage degradation experienced by the shielded solar cells and the aspect sensor was relatively small, being about 4 percent. In the absence of computed proton data for the orbit of Explorer XXIII, and because of the limitation in data accuracy of the telemetry and read-out systems, no conclusive explanation concerning the degradation of the shielded cells can be given. However, the amount of damage observed and the protection provided by the shield are substantiated by the performance of the primary power solar cells. Although the output of the power cells was not monitored, the power system voltages monitored during flight indicated no significant change at the end of 1 year in space. It is evident that the power solar cells, shielded in the same manner and degree as the shielded test groups, provided sufficient power for satisfactory operation of the electronic loads, and to maintain the batteries at a maximum capacity.

#### CONCLUDING REMARKS

The design objectives of the Explorer XXIII micrometeoroid satellite were successfully completed after 1 year in orbit. The results of the solar cell damage experiment show reasonable agreement with results of pre-flight radiation tests and with estimates made from electron and proton space distribution data. Output voltages of unshielded solar cells degraded approximately 16 percent of their initial values during 1 year in near-earth space. Voltage outputs of shielded cells degraded approximately 4 percent during this period. Variation in damage rates were observed with relatively

high decay periods occurring when apogee was in the southern hemisphere at latitudes associated with the southern anomoly. The protection provided by the synthetic fused silica shields indicate that the power solar cells should continue to operate satisfactorily for several more years in space.

1. Moon, P.: Proposed Standard Radiation Curves for Engineering Use. Jour. Franklin Institute. 230, 583 (1940).
2. Cunningham, F. G.: Earth-Reflected Solar Radiation Incident Upon Spherical Satellites in General Elliptical Orbits. NASA TN D-1472, February 1963, p. 232.
3. Vette, James I.: Models of the Trapped Radiation Environment. Vol. I: Inner Zone Protons and Electrons. NASA SP-3024, 1964, p. 27.
4. Cherry, William R. and Slifer, Luther W.: Solar Cell Radiation Damage Studies with 1 MeV Electrons and 4.6 MeV Protons. GSFC Report No. X-636-63-110, May 27, 1963.

# EXPLORER XXIII MICROMeteoroid SATELLITE

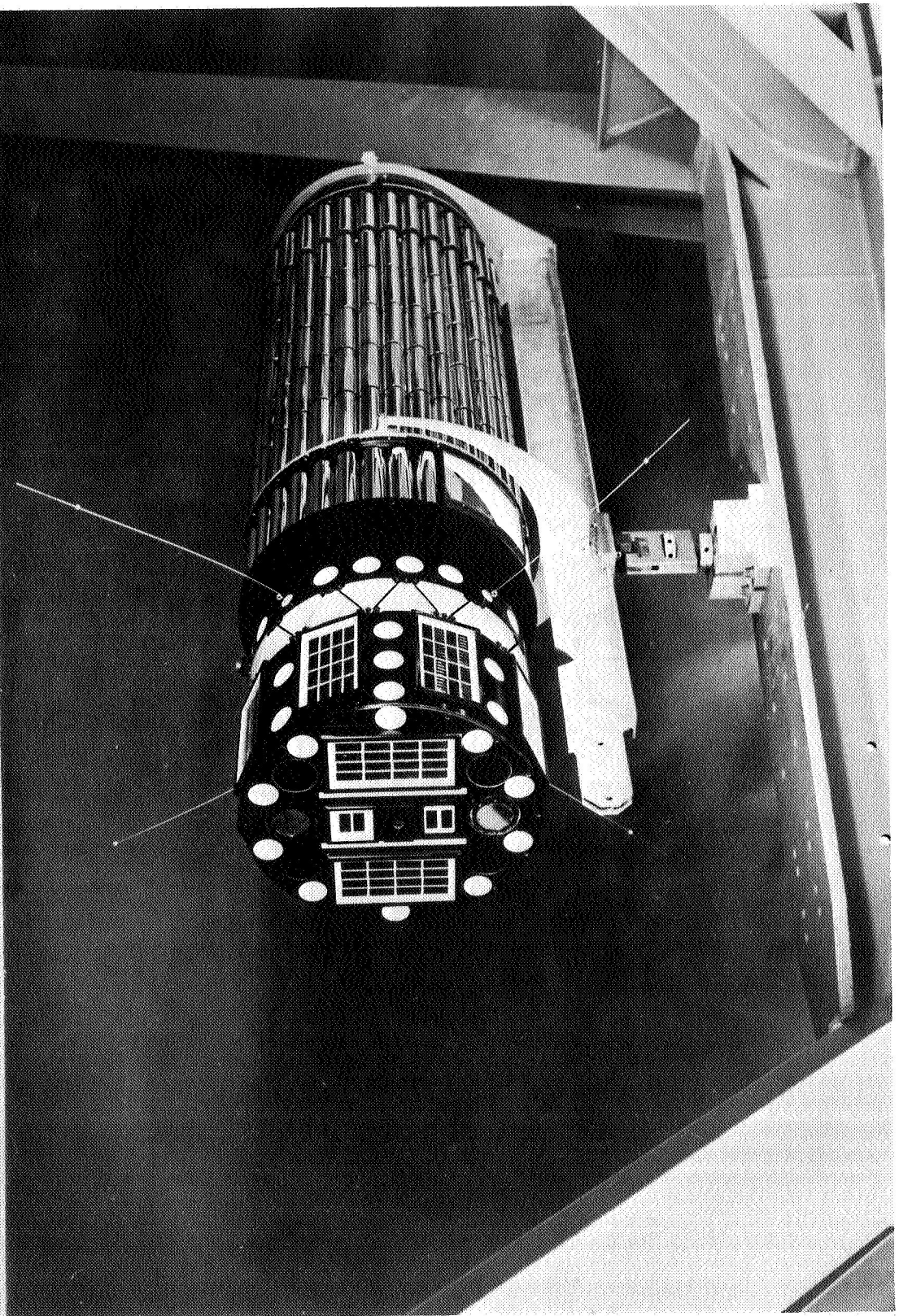
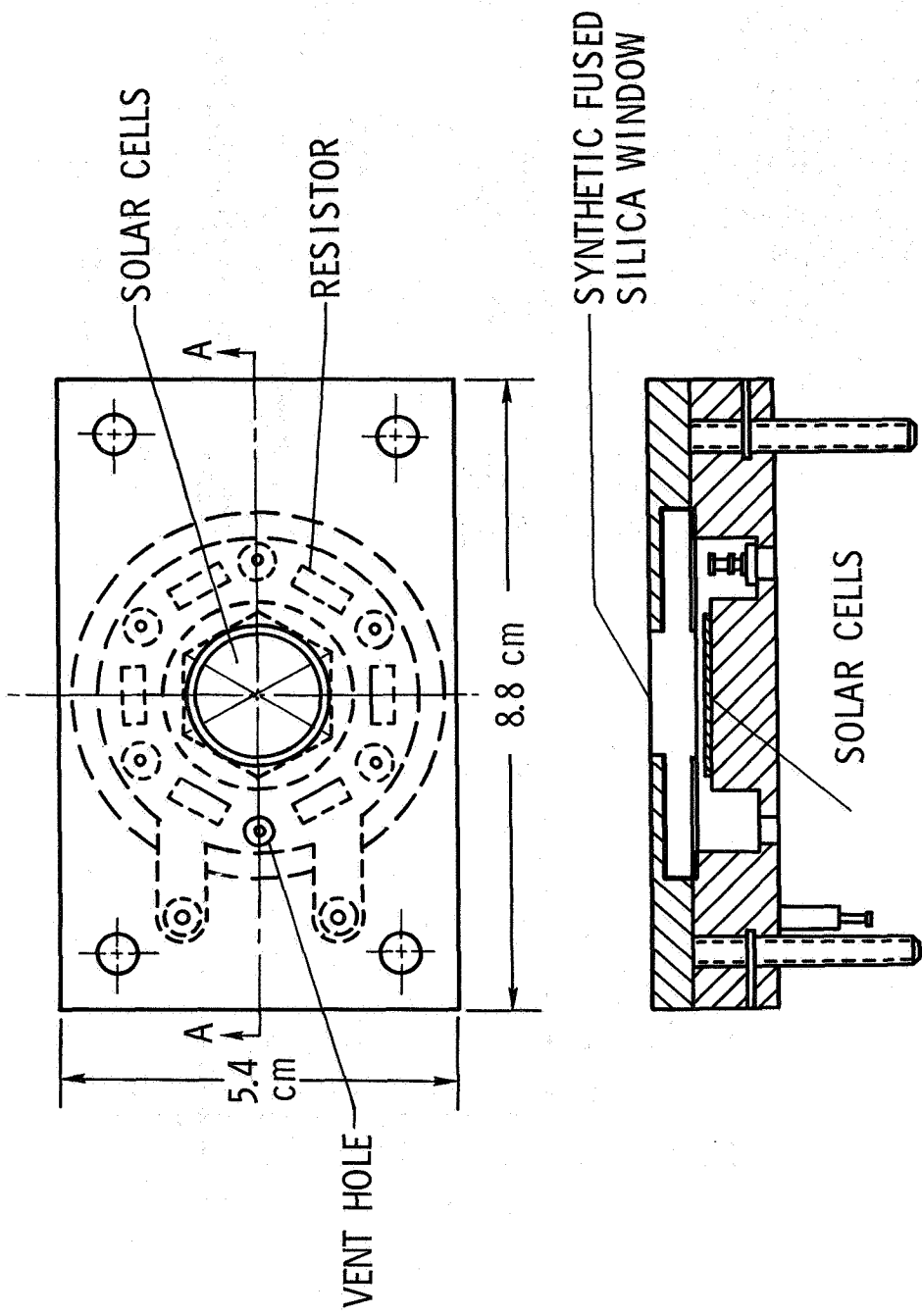


Figure 1

## SOLAR ASPECT SENSOR ASSEMBLY



SECTION A-A

Figure 2

# TEST SOLAR CELL ASSEMBLY

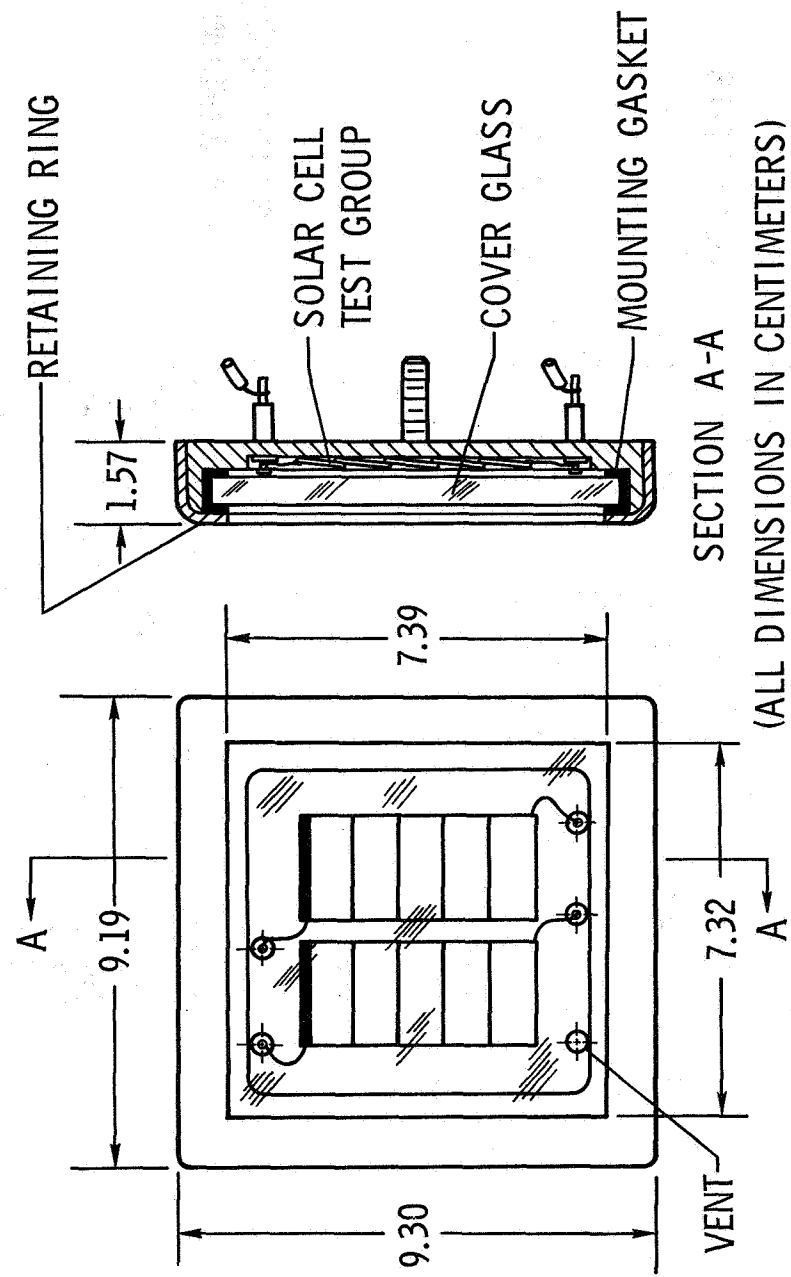


Figure 3

ANGULAR RESPONSE OF ASPECT SENSOR

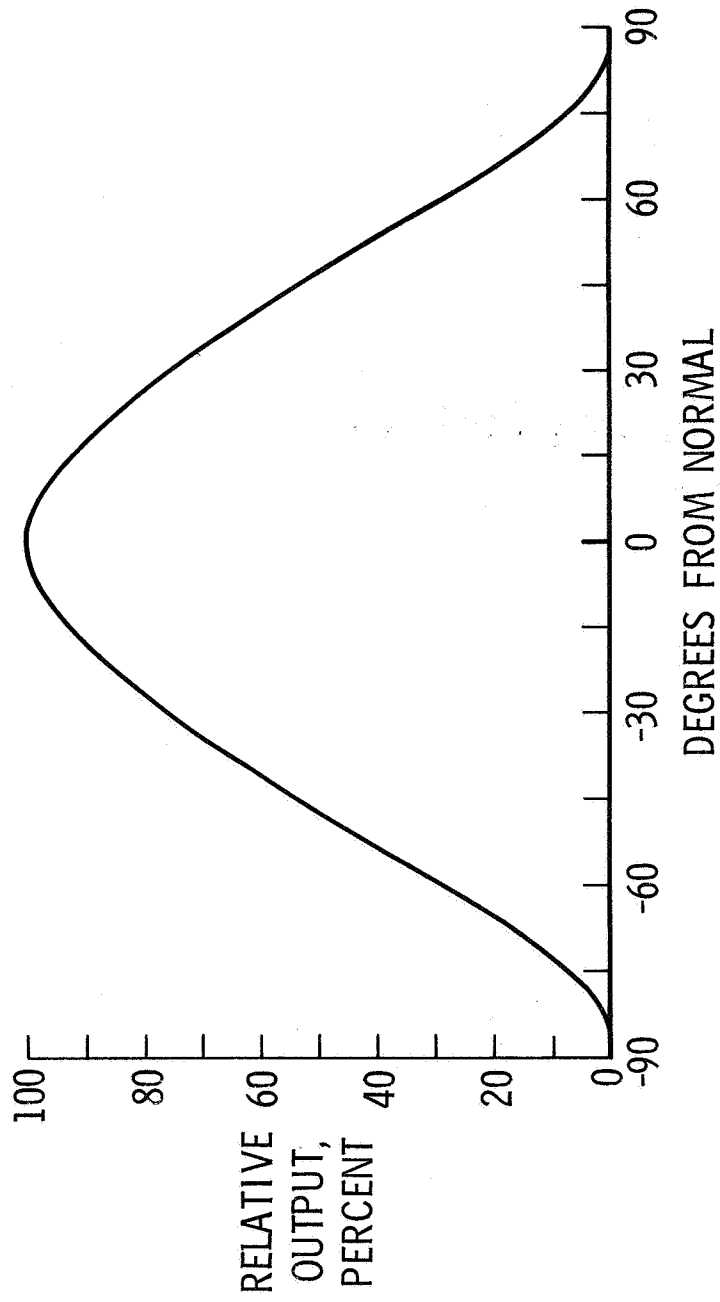


Figure 4

## ANGULAR RESPONSE OF TEST SOLAR CELL GROUPS

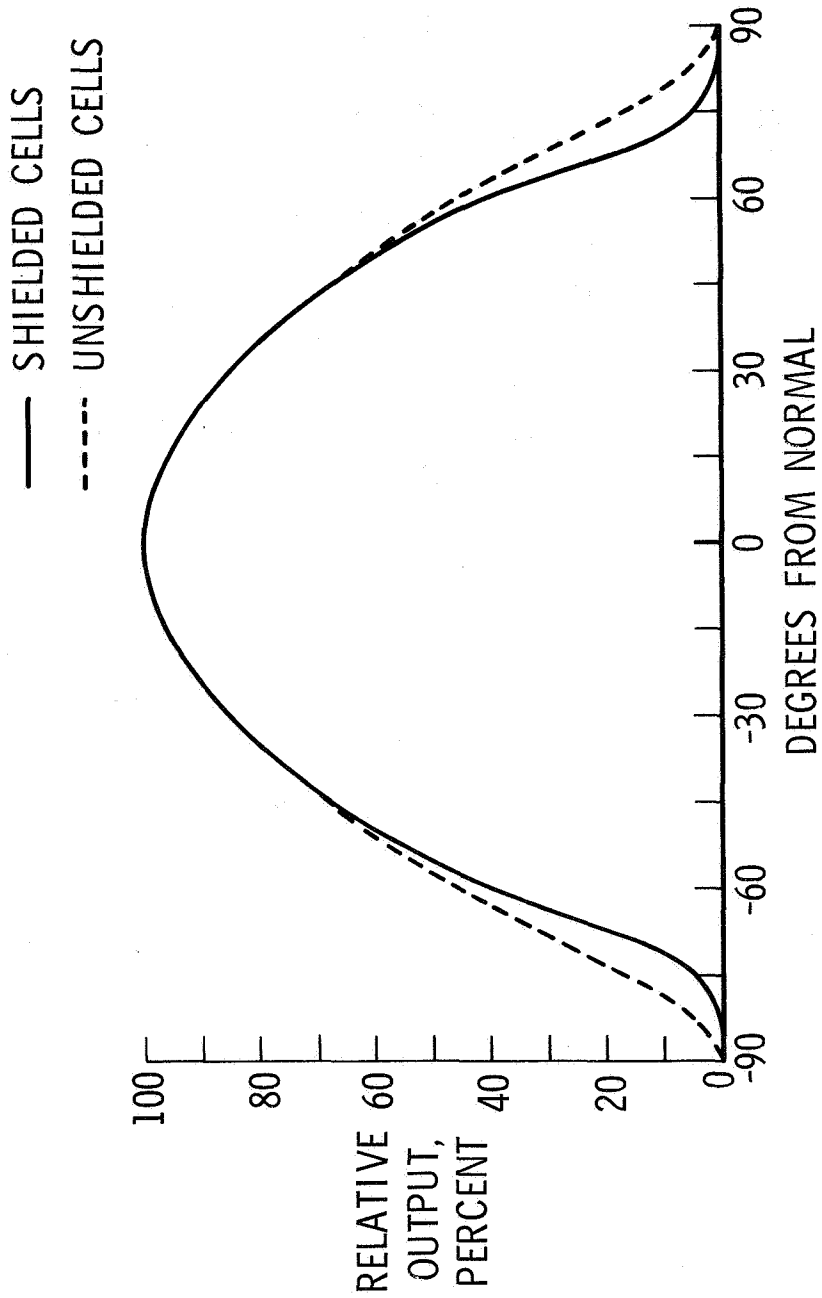


Figure 5

CALCULATED ORIENTATION OF MOMENTUM VECTOR  
RELATIVE TO SUN

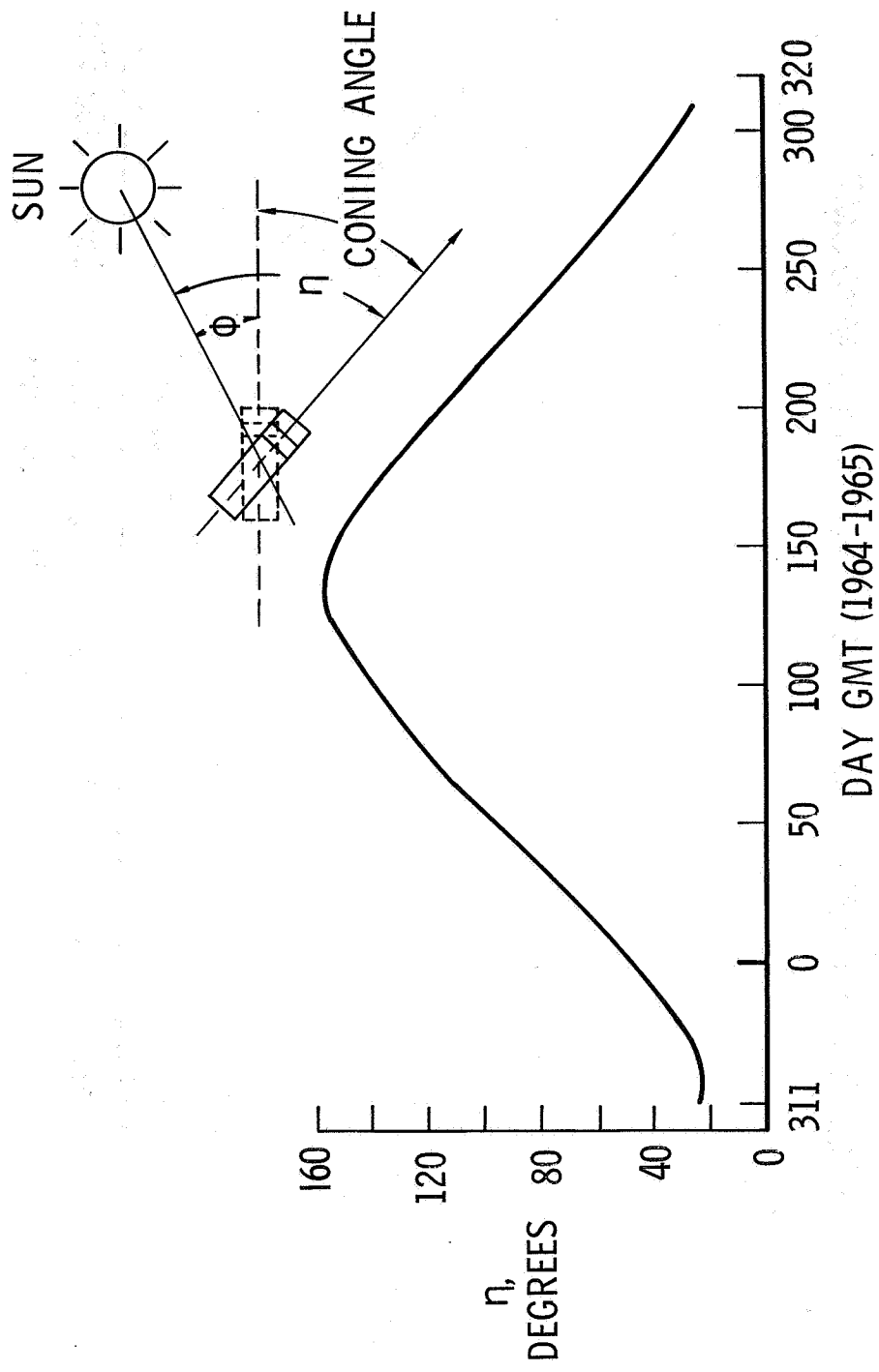


Figure 6

SOLAR CONSTANT VARIATION FROM 140 MW/CM<sup>2</sup>

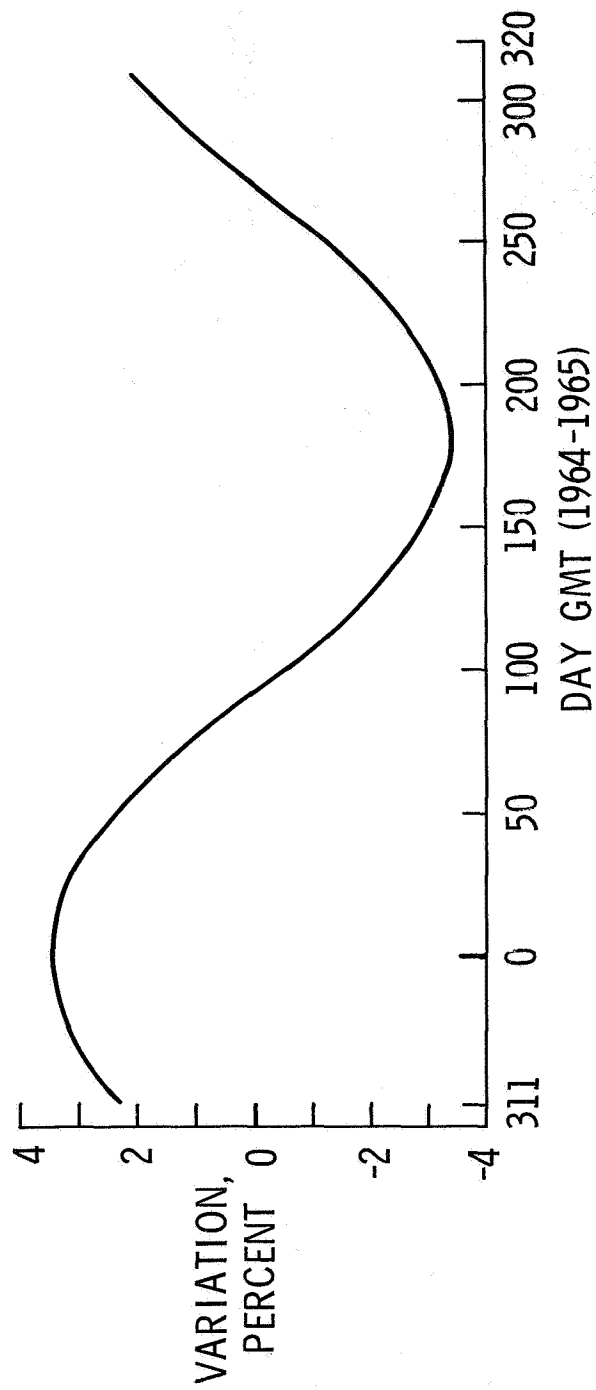


Figure 7

UNCORRECTED OUTPUT VOLTAGES DURING ORBIT NO. 336

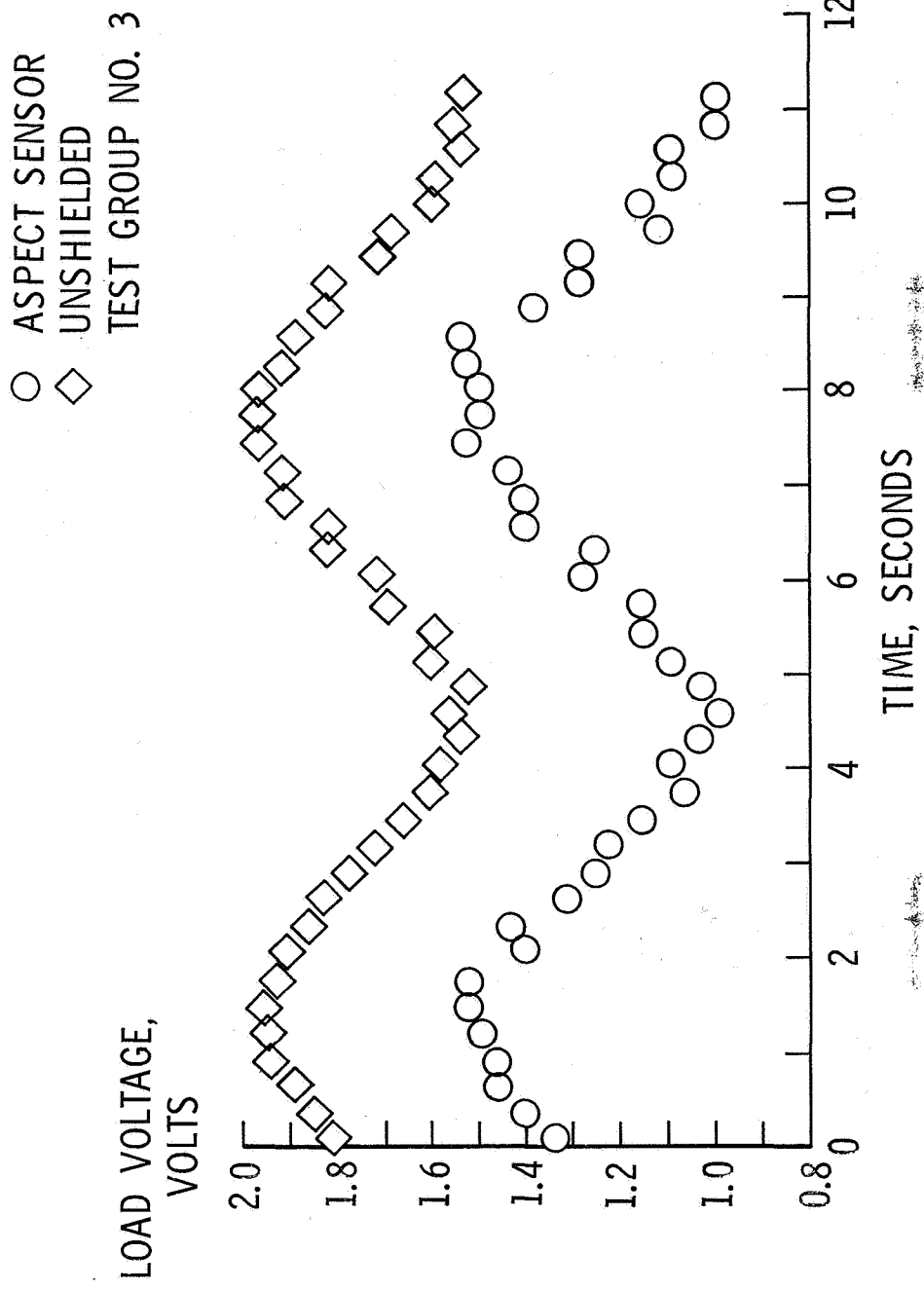


Figure 8

UNCORRECTED OUTPUT VOLTAGES DURING ORBIT NO. 3199

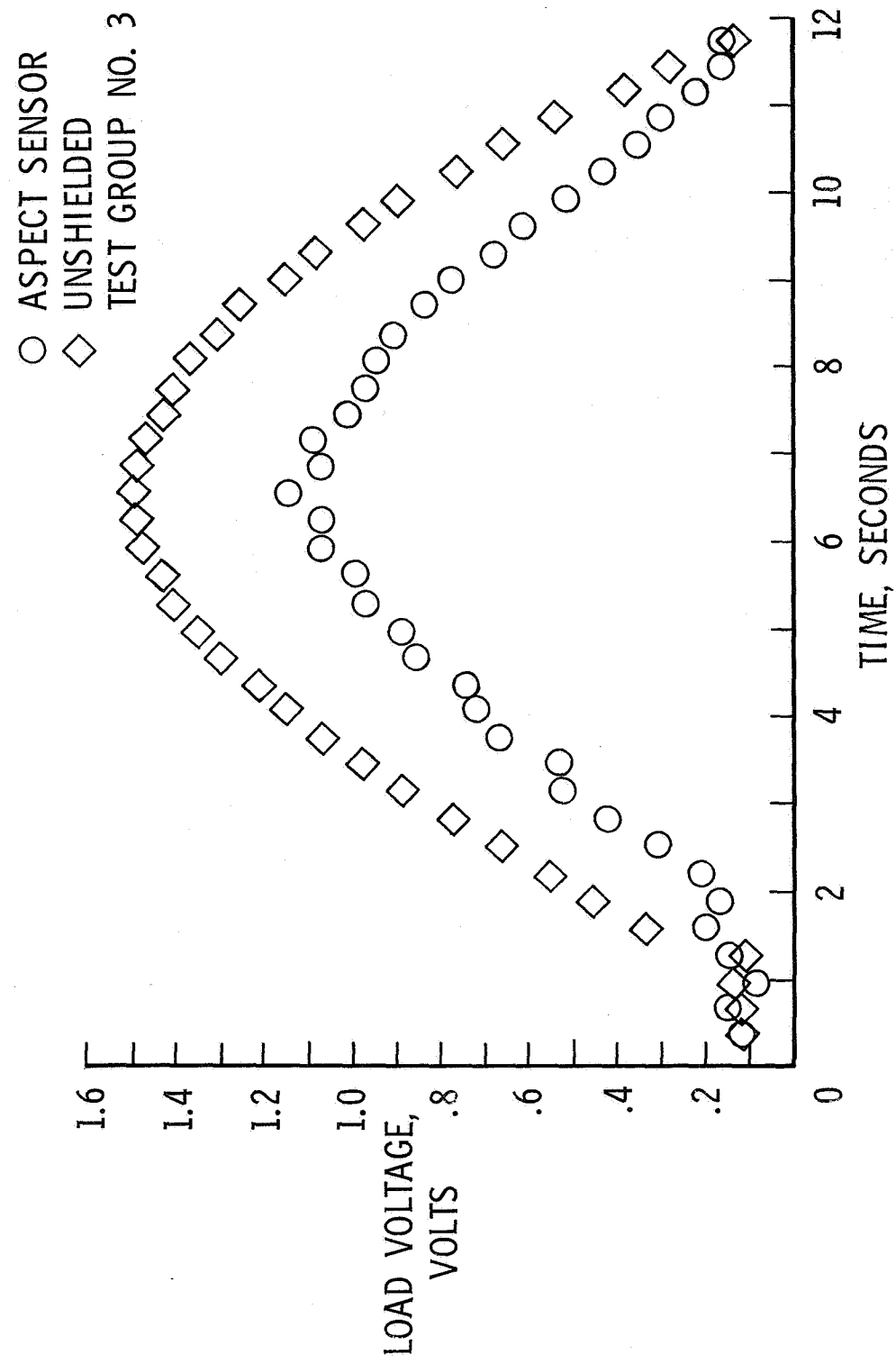
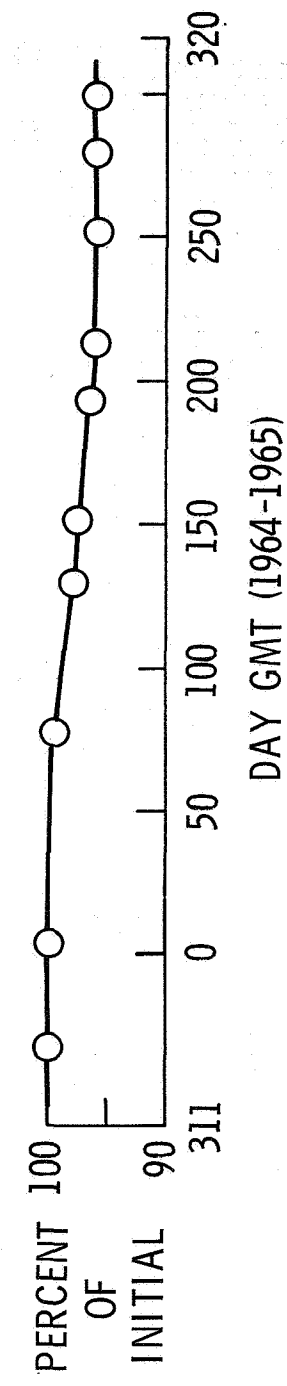


Figure 9

### NORMALIZED OUTPUT VOLTAGE OF ASPECT SENSOR



### ANGLE OF SOLAR INCIDENCE FOR SELECTED ORBITS

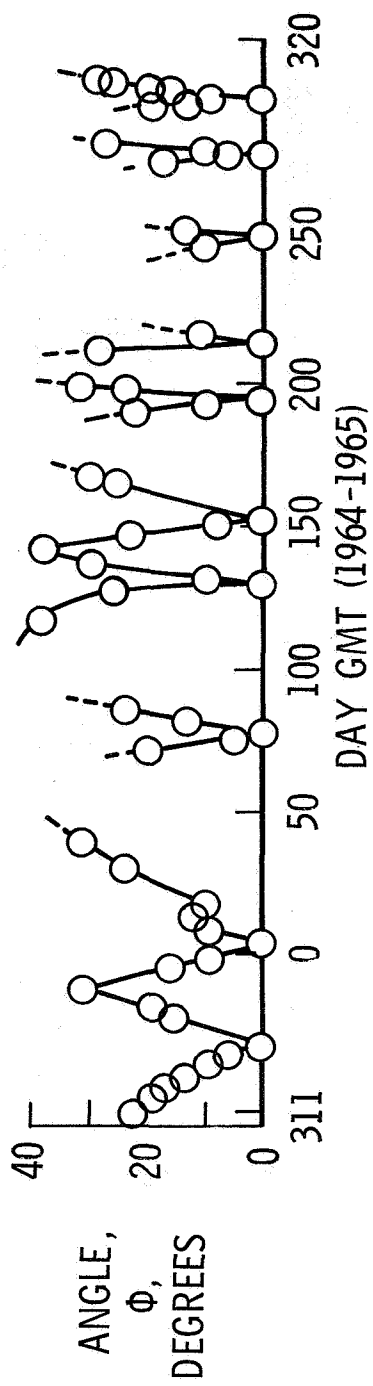


Figure 10

INTEGRATED ELECTRON FLUX PER ORBIT FOR EXPLORER XXXIII

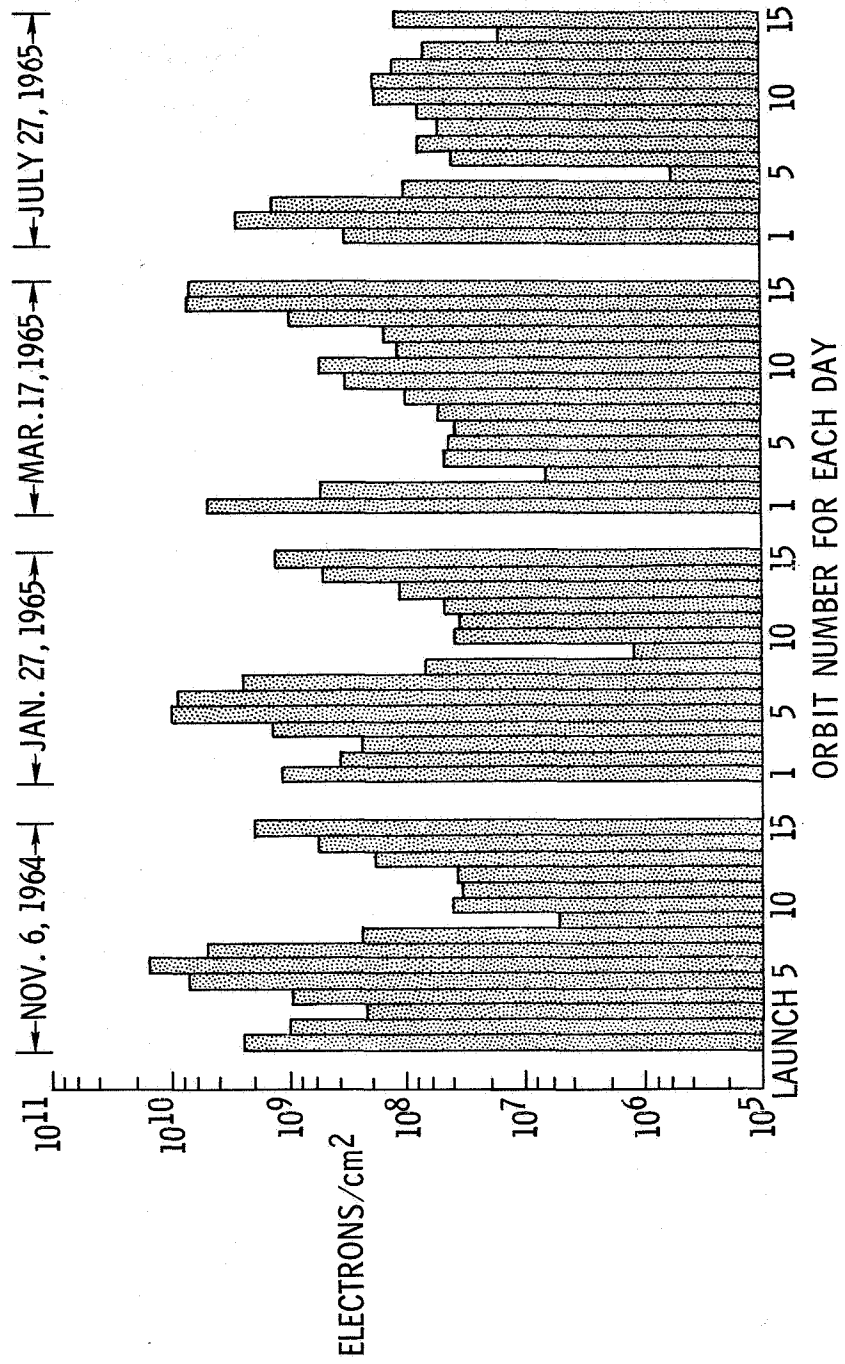


Figure 11

LATITUDE OF APOGEE FOR EXPLORER XXXIII

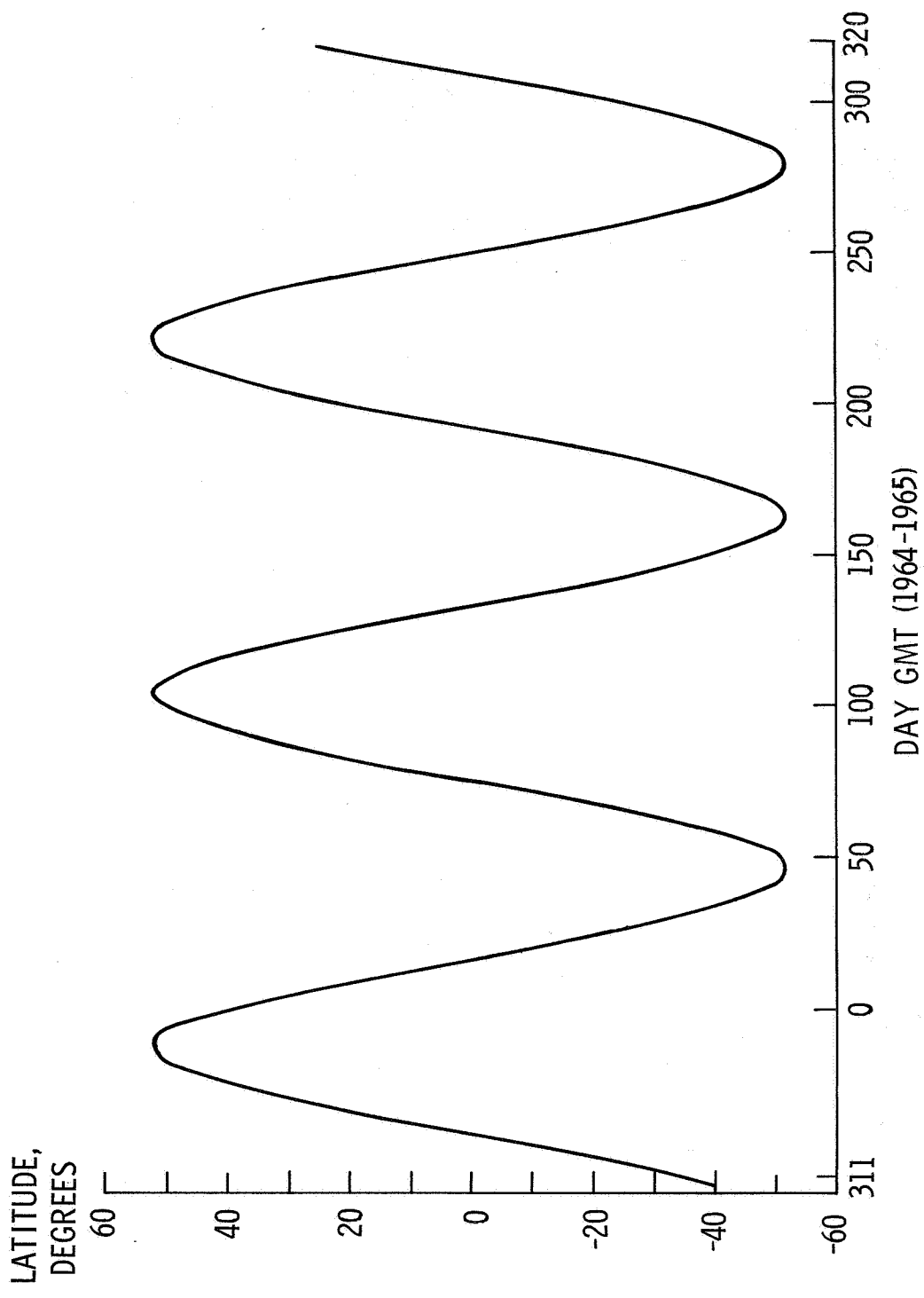


Figure 12

# VARIATION IN AVERAGE DAILY ELECTRON FLUX FOR EXPLORER XXXIII

TOTAL FLUENCE FOR YEAR:  $7.6 \times 10^{12} e/cm^2$   
AVERAGE FLUX RATE:  $2.1 \times 10^{10} e/cm^2/day$

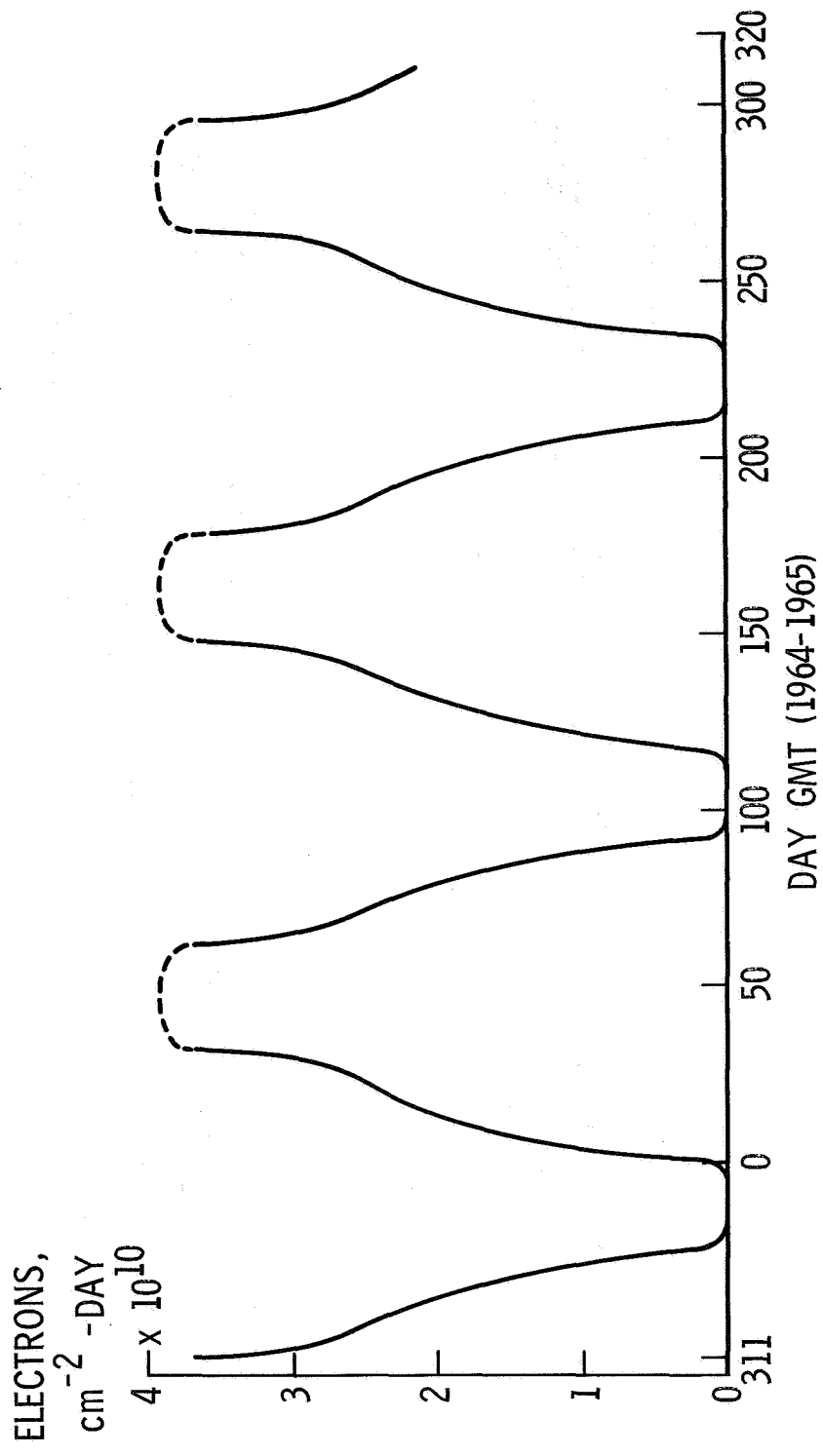


Figure 13

## DEGRADATION OF TEST SOLAR CELLS

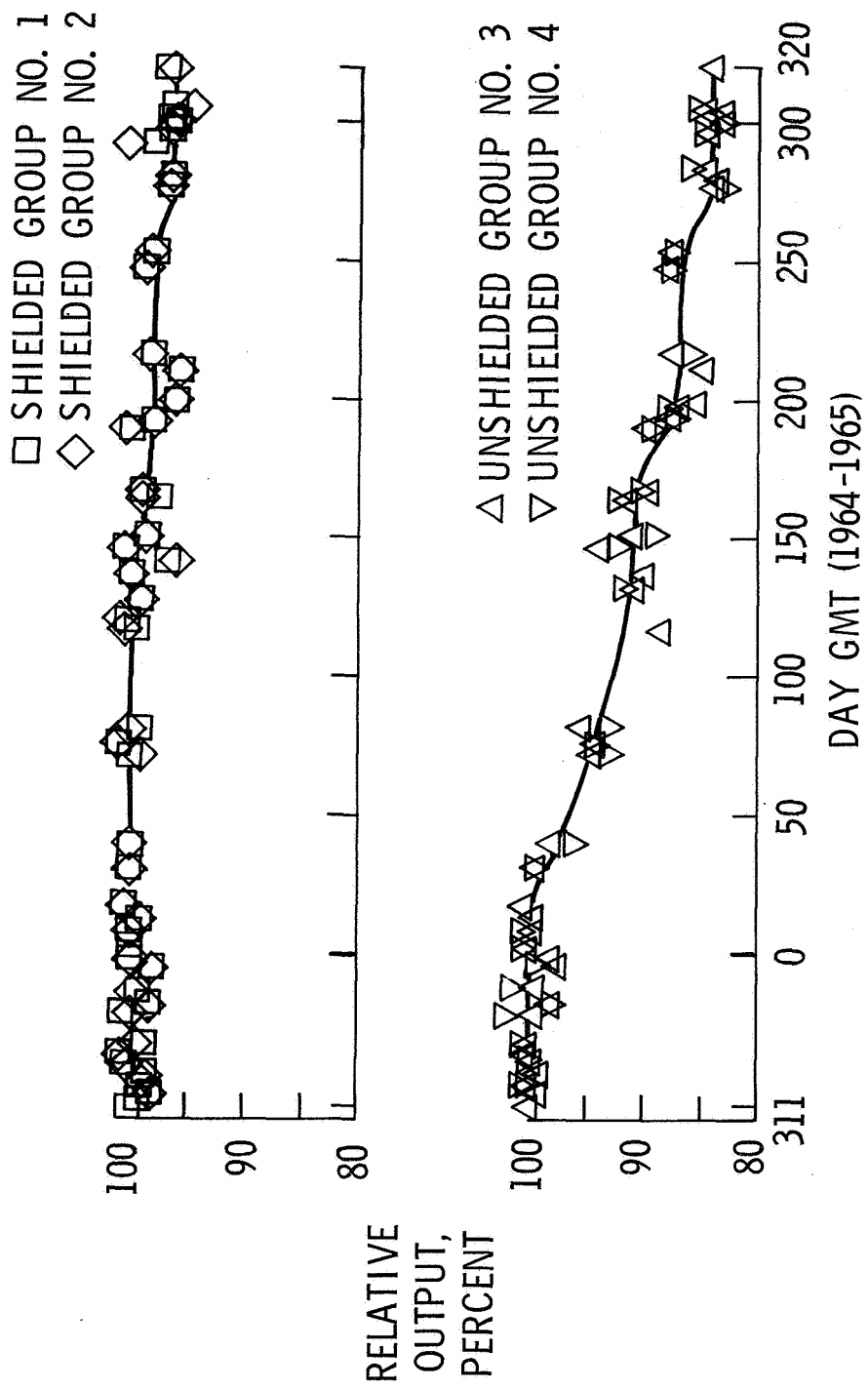


Figure 14